



## Performance Comparison of Face Recognition Algorithms based on face image Retrieval

Hicham Mokhtari<sup>1</sup>, Idir Belaidi<sup>2</sup> and Said Alem<sup>1</sup>

<sup>1</sup>Laboratory of Solid Mechanics and Systems, Faculty of science and engineering, University of M'hamed Bougara Boumerdés, ALGERIA

<sup>2</sup>Laboratory of Energetic, Mechanics and Engineering, Faculty of science and engineering, University of M'hamed Bougara Boumerdés, ALGERIA

Available online at: [www.isca.in](http://www.isca.in), [www.isca.me](http://www.isca.me)

Received 25<sup>th</sup> January 2013, revised 1<sup>st</sup> April 2013, accepted 28<sup>th</sup> June 2013

### Abstract

Biometric systems are complex systems of safety measures based on physical, biological and the humans behavioral. The automatic face recognition has become a highly active research area, mainly due to numbers published papers in recent years. In this paper, we present a comparative study for evaluation of face recognition system based on face restoration. Our study is performed in two consecutive steps, In the first step, we use two methods of image restoration called Centralized sparse representation (CSR) and adaptive sparse domain selection with adaptive regularization (ASDS-AR) while in the second step the set of methods that have been used are principal component analysis (PCA), linear discriminant analysis (LDA) kernel principal component analysis (KPCA) and Kernel Fisher Analysis (KFA) for face recognition and we associated the Gabor Wavelets and Phase Congruency in order to achieve the evaluation of our proposed model. In addition, the comparative analysis on the ORL database is also employed in the experiments to evaluate the susceptibility of the appearance based methods on various image degradations which can occur in "real-life" operating conditions. Our experimental results suggest that Gabor linear discriminant analysis (GLDA) ensures the most consistent verification rates across the tested ORL databases for both methods CSR and ASDS-AR.

**Keywords:** Face recognition, centralized sparse representation, adaptive sparse domain selection and adaptive regularization, image deblurring, ORL databases.

### Introduction

Biometrics is a scientific discipline that is based on the measurement of physical, biological and behavioral human characteristics that can be processed to identify.

Among the different characteristics suitable for biometric recognition, the face recognition, this modality is one of the most active research areas in the field of biometrics seen their application field such as smart surveillance, access and border control using in e-government, e-health and e-commerce service.

Current systems face recognition may have good results in relatively controlled environments. However, the algorithms developed are very effective over a wide range of viewpoints, occlusions, aging of subjects and complex outdoor lighting is always an important area of research<sup>1</sup>.

Other factors that also affect the performance of face recognition systems include blur that can cause significant image degradation. Blur is unfortunately often present in face images and is usually due to camera movement, it affects the appearance of faces in images, causing a blur on the appearance of the face of the person who has changed drastically<sup>2</sup>.

Many researchers have tackled the problem of face image deblurring such as adaptive unsharp masking by Romponi and Polesel<sup>3,4</sup> regularized image deconvolution<sup>5</sup> restoration of face image<sup>6</sup>. Moreover, there are several methods for face recognition such as principal component analysis (PCA), linear discriminant analysis (LDA), kernel principal component analysis (KPCA), Gabor-based kernel partial-least-squares discrimination (GKPLSD) and Complete Gabor Fisher Classifier (CGFC)<sup>7,8</sup>.

In this paper, a comparative analysis of the performance of face recognition system is performed in two consecutive steps, In the first step, we use two methods of image restoration called Centralized sparse representation (CSR) and adaptive sparse domain selection with adaptive regularization (ASDS-AR) while in the second step the set of methods that have been used are principal component analysis (PCA), linear discriminant analysis (LDA) kernel principal component analysis (KPCA) and Kernel Fisher Analysis (KFA) for face recognition and we associated the Gabor Wavelets and Phase Congruency in order to achieve the evaluation of our proposed model. We conduct face verification experiments using the ORL database which lead to evaluate the sensitivity of methods based on the appearance of image degradation using Centralized sparse

representation (CSR) and Adaptive sparse domain selection with adaptive regularization (ASDS -AR) for image deblurring. The rest of the paper is structured as follows. Section II introduces the basic concept of Gabor Wavelet and Phase Congruency. Section III describes the employed ORL databases. Section IV, presents the image deblurring using two methods CSR and ASDS-AR. In section V, we present our proposed model. Section VI presents the experiments and corresponding results, while the last section concludes the paper.

## Algorithms

For face recognition, we used well known appearance based methods: PCA, LDA, KPCA and KFA. The four methods reduce the high dimension image to a smaller dimension which is more appropriate for presentation of the face image.

**Principal Component Analysis (PCA):** The Principal Component Analysis (PCA) is very used in face recognition, is a powerful algorithm based feature extraction technique, which applies the Karhunen-Loéve transform to a set of training images and derives a number of projection axes that act as the basis vector for the PCA subspace. All images of known faces are projected onto the face space to find set of weights that describe the contribution of each vector. For identify an unknown person, his normalized image is first projected onto face space to achieve its set of weights. Than we compare these weights to sets of weights of known persons from the data bases. If we consider the image elements are the random variables, the PCA basis vectors are defined as eigenvectors of scatter matrix  $S_T$ :

$$S_T = \sum_{i=1}^m (x_i - \mu)(x_i - \mu)^T \quad (1)$$

Where  $\mu$  is the mean of all images in the training set.  $x_i$  is the  $i$ -th image with its columns concatenated in a vector and  $M$  is the number of all training images. The projection matrix  $W_{PCA}$  is composed of  $m$  eigenvectors corresponding to  $m$  eigenvalues of scatter matrix  $S_T$ , thus creating an  $m$  dimensional face space. Since these eigenvectors (PCA basis vectors) look like some ghostly faces they were conveniently named eigenfaces.

**Linear Discriminant Analysis (LDA):** Unlike the principal components analysis PCA, which considers only the variance of the training images to construct a subspace; linear discriminant analysis (LDA) aims at improving upon PCA by also taking the class-membership information of the training images into account when seeking for a subspace. So, the LDA method finds the vectors in the underlying space that best discriminate among classes. For all samples of all classes it defined two matrixes: between-class scatter matrix  $S_B$  and the within-class scatter matrix  $S_w$ .  $S_B$  Represents the scatter of features around the overall mean  $\mu$  for all face classes and  $S_w$  represents the scatter of features around the mean of each face class<sup>9</sup>:

$$S_B = \sum_{i=1}^c M_i (\mu_i - \mu)(\mu_i - \mu)^T \quad (2)$$

$$S_w = \sum_{i=1}^c \sum_{x_k \in X_i} (x_k - \mu_i)(x_k - \mu_i)^T \quad (3)$$

Where  $M_i$  is the number of training samples in class  $i$ ,  $c$  is the number of distinct classes,  $\mu_i$  is the mean vector of samples belonging to class  $i$  and  $X_i$  represents the set of samples belonging to class  $i$  with  $x_k$  being the  $k$ -th image of that class. The goal of to maximize  $S_B$  while minimizing  $S_w$ , in other word, maximize the ratio  $\left(\frac{\det|S_B|}{\det|S_w|}\right)$ . This ratio is maximized when

the column vectors of projection matrix ( $W_{LDA}$ ) are the eigenvectors of  $S_w^{-1} \cdot S_B$ .

To prevent singularity of the matrix  $S_w$  PCA is used as preprocessing step and the final transformation is  $W_{opt} = W_{PCA} \cdot W_{LDA}$ .

**Kernel principal component analysis (KPCA):** KPCA main technique is calculating PCA onversion in a mapping space by a Non-linear mapping function which for estimating this mapping, kernel idea is used. Consider  $\varphi(X_1), \dots, \varphi(X_N)$  are mapped data which their mean is not zero. First mapped data mean becomes zero following formula<sup>10</sup>:

$$\hat{\varphi}(X_k) = \varphi(X_k) - \frac{1}{N} \sum_{j=1}^n \varphi(X_j) \quad (4)$$

Covariance matrix is calculated by (5) formula:

$$\hat{\Sigma} = \frac{1}{N} \sum_{j=1}^n \hat{\varphi}(X_j) \hat{\varphi}(X_j)^T \quad (5)$$

$\hat{\lambda}\hat{V} = \hat{\Sigma}\hat{V}$  is special quantity equation for covariance matrix where  $\lambda \geq 0$  is special quantity and  $\hat{V} \in F \setminus \{0\}$  i.e F except  $\{0\}$  is special vectors. Special vectors equation equivalent can be written in the form of (6) formula:

$$\hat{\lambda}(\hat{\varphi}(X_k)\hat{V}) = (\hat{\varphi}(X_k)\hat{\Sigma}\hat{V}), k = 1, \dots, N \quad (6)$$

Where  $\alpha_k$  are coefficients which their quantities are selected in way that (9) formula is established.

$$\hat{V} = \sum_{k=1}^N \hat{\alpha}_k \hat{\varphi}(X_k) \quad (7)$$

Where by substituting (7) formula by (6) formula we have:

$$\hat{\lambda}\hat{\alpha} = K\hat{\alpha}, (\hat{\alpha} = (\alpha_1, \dots, \alpha_N)^T) \quad (8)$$

Where  $K$  is kernel matrix which is in the form of  $N \times N$  square matrix by  $K_{i,j} = (\varphi(X_i), \varphi(X_j)) = k(X_i, X_j)$  elements. For  $(\lambda_k, \alpha^k)$  solution normalization,  $\lambda_k(\lambda_k, \alpha^k) = 1$  formula is applied in mapping space, also like every other PCA algorithms, data should be concentrated in mapped space, so kernel matrix should be replaced by following formula:

$$\hat{K} = K - \mathbf{1}_N K - K \mathbf{1}_N + \mathbf{1}_N K \mathbf{1}_N \quad (9)$$

$$\text{Where } (\mathbf{1}_N)_{i,j} = \frac{1}{N}$$

**Kernel fisher analysis (KFA):** The main idea of this method is to yield a nonlinear discriminant analysis in the higher space. The input data is projected into an implicit feature space by nonlinear mapping,  $\Phi : x \in R^N \rightarrow f \in F$  then seek to find a nonlinear transformation matrix, which can maximize the between-class scatter and minimize the within class scatter<sup>11</sup>. First, we define the dot product in  $F$  as following.

$$k(x, y) = \Phi(x) \cdot \Phi(y) \quad (10)$$

Between-class scatter matrix  $S_B$  and within class scatter matrix  $S_w$  are defined in the feature space  $F$ :

$$S_w = \sum_{i=1}^C p(w_i) E((\Phi(x) - u)(\Phi(x) - u)^T) \quad (11)$$

$$S_B = \sum_{i=1}^C p(w_i) E(u_i - u)(u_i - u)^T \quad (12)$$

$u_i$  Denotes the samples mean of class  $i$  and  $u$  denote mean of all the samples in  $F$ ,  $p(w_i)$  is the prior probability.

## Gabor Wavelets

Gabor wavelets were introduced to image analysis because of their similarity to the receptive field profiles in cortical simple cells. They characterize the image as localized orientation selective and frequency selective features. Therefore, low level features, such as peaks, valleys and ridges are enhanced by 2-D Gabor filters. Thus, the eyes, nose and mouth, with other face details like wrinkles, dimples and scars are enhanced as key features to represent the face in higher dimensional space. Also, the Gabor wavelet representation of face image is robust to misalignment to some degree because it captures the local texture characterized by spatial frequency, spatial position and orientation.

The commonly used Gabor filter is defined as follows<sup>12</sup>:

$$w_{u,v}(z) = \frac{\|k_{u,v}\|^2}{\sigma^2} e^{-\frac{\|k_{u,v}\|^2 \|z\|^2}{2\sigma^2}} \begin{bmatrix} ik_{u,v} z & -\frac{\sigma^2}{2} \\ e^{ik_{u,v} z} & -e^{-\frac{\sigma^2}{2}} \end{bmatrix} \quad (13)$$

Where  $u$  and  $v$  define the orientation and scale index of the Gabor kernels,  $z = [x, y]^T$ ,  $\|\cdot\|$  is the norm operator, and the wave vector  $k_{u,v}$  is defined below.

$$k_{u,v} = k_v e^{i\phi_u} \quad (14)$$

$$\text{Where } k_v = \frac{k_{\max}}{f^v} \text{ and } \phi_u = \frac{\pi u}{8} \text{ with } k_{\max} \text{ the maximum}$$

frequency, and  $f$  being the spacing factor between kernels in the frequency domain. The term  $e^{-\frac{\sigma^2}{2}}$  is subtracted to render the filters insensitive to the overall level of illumination. In face recognition, researchers commonly use 40 Gabor wavelets with five scales  $v \in [0, 5]$  and eight orientations  $u \in [0, 8)$  with  $\sigma = 2\pi$ ,  $f = \sqrt{2}$  for half octave spacing  $k_{\max} = \frac{\pi}{2}$  for 128x128 images size and  $k_{\max} = \pi$  for 64x64 images size.

Gabor image,  $G_{u,v}(z) \in C$ , is generated by taking the convolution of face image,  $I(z)$  and Gabor wavelet,  $w_{u,v}(z)$ . The convolution process can be taken in the Fourier domain for fast computation. In the face recognition community, many researchers<sup>13-17</sup> have widely used the magnitude of Gabor filters for face representation. Here 5 frequencies and 8 orientations are used, figure 1 shows the 40 Gabor Kernels in equation 13 used by us.

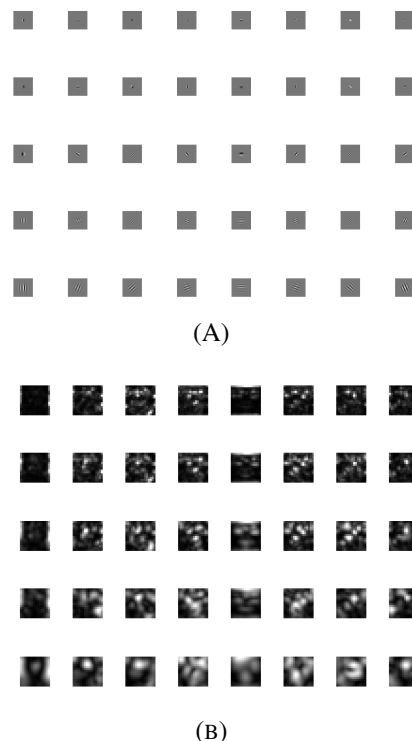


**Figure-1**  
“A” is the real part of 40 Gabor Kernels, “B” is the magnitude of Gabor faces

## Phase Congruency Model

The phase congruency model as proposed by Hong<sup>18</sup> in purpose to detect the angles and the robust edges in digital image. The phase congruency model is relatively a new model. It's applied in several domain of image processing like: face alignment<sup>19</sup>, noise removal for iris image<sup>20</sup>, feature extraction of chromosomes<sup>21</sup>. From the above, the phase congruency represents a robust and accurate model for features extraction in the wide ranges of images. The phase congruency was developed with the goal of robust edge and corner detection in digital images. Unlike classical gradient-based edge detectors, which search for image points of maximum intensity gradients and are known to be susceptible to image contrast and illumination conditions, the phase congruency model searches for points of order in the frequency spectrum, and provides an illumination invariant model of edge detection. For 1D signals, the phase congruency  $PC(x)$  is defined implicitly by the relation of the energy at a given point in the signal  $E(x)$  and the sum of the Fourier amplitudes  $A_n$  as shown by Venkatesh<sup>22</sup>:

$$E(x) = PC(x) \sum_n A_n \quad (15)$$

Where  $n$  denotes the number of Fourier components. Thus, phase congruency at a given location of the signal  $x$  is defined as the ratio of the local energy at this location and the sum of Fourier amplitudes. Kovesi extended the above concept to 2D signals by computing the phase congruency with logarithmic Gabor filters using the following expression:

$$PC_{2D}(x, y) = \frac{\sum_{v=0}^{r-1} \sum_{u=0}^{p-1} A_{u,v}(x, y) \Delta\Phi_{u,v}(x, y)}{\sum_{v=0}^{r-1} \sum_{u=0}^{p-1} A_{u,v}(x, y) + \epsilon} \quad (16)$$

Where  $A_{u,v}(x, y)$  denotes the magnitude response of the logarithmic Gabor filter at scale  $u$  and orientation  $v$ ,  $\epsilon$  represents a small constant that prevents divisions with zero, and  $\Delta\Phi_{u,v}(x, y)$  stands for a phase deviation measure defined as:

$$\Delta\Phi_{u,v}(x, y) = \cos(\phi_{u,v}(x, y) - \bar{\phi}_v(x, y)) - |\sin(\phi_{u,v}(x, y) - \bar{\phi}_v(x, y))| \quad (17)$$

Here  $\phi_{u,v}(x, y)$  denotes the phase angle of the logarithmic Gabor filters at the  $u$  th scale and  $v$  th orientation, while  $\phi_v(z)$  represents the mean phase angle at the  $v$ th orientation. At closer examination of the 2D phase congruency model we can notice that it first computes the phase congruency for each of the employed filter orientations and subsequently combines the results to form the final output. The following figure 2 represents a phase congruency feature for all (eight) filters orientation.

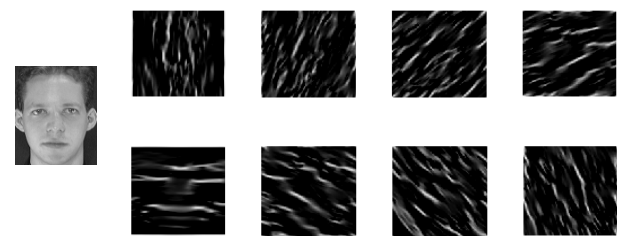


**Figure-2**  
**Phase Congruency feature for all filter orientation**

## Image Restoration

The objective of restoration is to improve a given image in some predefined sense. Although there are areas of overlap between image enhancement and image restoration, the former is largely a subjective process, while image restoration is for the most part an objective process. Restoration attempts to reconstruction or recover an image that has been degraded by using a priori knowledge of the degradation phenomenon. Thus, restoration techniques are oriented toward modeling the degradation and applying the inverse process in order to recover the original image.

This approach usually involves formulating a criterion of goodness that yields an optimal estimate of the desired result. By contrast, enhancement techniques basically are heuristic procedures designed to manipulate an image in order to take advantage of the psychophysical aspects of the human visual system. For example, contrast stretching is considered an enhancement technique because it is based primarily on the pleasing aspects it might present to the viewer, whereas removal of image blur by applying a deblurring function is considered a restoration technique<sup>23</sup>.

In our study, we use two methods for image deblurring. The centralized sparse representation (CSR) and adaptive sparse domain selection with adaptive regularization.

**Centralized Sparse Representation (CSR):** A new concept was proposed by W. Dong et al.<sup>24</sup>, this model is called centralized sparse representation (CSR), the CSR model is in the way to take its place and prove its efficiency in image processing, and more precisely in image restoration.

The main procedures of the CSR based image restoration algorithm are summarized in the following algorithm. In the CSR model, there are two parameters,  $\lambda$  and  $\gamma$ , which balance the local redundancy induced sparsity and the nonlocal redundancy induced sparsity, respectively. In this case, we must calculate  $\lambda$  and  $\gamma$  using equation (18):

$$\gamma_i = \frac{2\sqrt{2}}{\delta_i} \sigma_n^2 \quad ; \quad \lambda_i = \frac{2\sqrt{2}}{\sigma_i} \sigma_n^2 \quad (18)$$

### The Main algorithm of Centralized Sparse Representation:

**Step 1:** *Initialization:* Compute an initial estimate  $\hat{x}$  using the standard sparse model.

**Step 2:** *Outer loop:* iterate on  $l = 1, 2 \dots L$ . i. Update the dictionary for each cluster of similar patches by using PCA, ii. Update the regularization parameters ( $\lambda$  and  $\gamma$ ) using equation (1), iii. Calculate the nonlocal means  $\mu_i^{(l-1)}$  from the sparse codes  $\alpha_y^{(l-1)}$ , iv. Calculate  $\alpha_y^{(l)}$  via the extended iterative shrinkage algorithm<sup>25</sup>.

**Adaptive sparse domain selection and adaptive regularization:** The adaptive sparse domain selection and adaptive regularization method was proposed by Dong<sup>26</sup> which is used for recovering degraded images, by suggesting a novel sparse representation based image deblurring and (single image) super-resolution method using adaptive sparse domain selection (ASDS) and adaptive regularization (AR). The ASDS-AR improves significantly the effectiveness of sparse modeling. In our case, we used it for face deblurring.

**ORL Databases:** The ORL database was acquired at AT&T Laboratories Cambridge University Computer laboratory. The ORL Database contains a set of face images taken between April 1992 and April 1994 at the lab. The database was used in the context of face recognition.

There are ten different images of each of 40 distinct subjects. For some subjects, the images were taken at different times, varying the lighting, facial expressions (open / closed eyes, smiling / not smiling) and facial details (glasses / no glasses). All the images were taken against a dark homogeneous background with the subjects in an upright, frontal position (with tolerance for some side movement). The files are in PGM format. The size of each image is 92x112 pixels, with 256 grey levels per pixel. The images are organized in 40 directories (one for each subject). In each of these directories, there are ten different images of that subject, which have names of the form Y.pgm, where Y is the image number for that subject (between 1 and 10).

**Proposed Model:** We first, use the original image. Then, after using the original base, for two cases, first, we due to a soft movement (9x9 Uniform blur  $\sigma_n = \sqrt{2}$ ), in the second, we put together a soft movement with a noise (Gaussian blur with standard deviation 3). Consequently, we use the centralized sparse representation (CSR) and adaptive sparse domain selection with adaptive regularization (ASDS-AR), together, permits us to get back regain and restore the degraded faces images, least but not last, the obtain result of the former step and the technique of recognition of faces allows us to evaluate the system. Figure 3 represent the different steps of our proposed model.

### Experiments and Discussion

To evaluate the performance of all algorithms, we conduct experiments on ORL Database based on image face deblurring (9x9 uniforms blur  $\sigma_n = \sqrt{2}$  and Gaussian blur with standard deviation 3,  $\sigma_n = \sqrt{2}$ ) using centralized sparse representation (CSR) and adaptive sparse domain selection with adaptive regularization (ASDS-AR). Recognition rate and equal error rate of KFA, KPCA, LDA, PCA, GKFA, GKPCA, GLDA, GPCA, PCKFA, PCKPCA, PCLDA and PCPCA are compared.

**Recognition experiments:** In this section, we present the experimental results obtained with the restoration of image ORL Databases. In our study, we use two methods the Centralized sparse representation CSR and the adaptive sparse domain selection with adaptive regularization ASDS-AR. Our model is based on blur faces. We used two types of blur kernels, a Gaussian kernel of standard deviation 3 and a 9x9 uniform kernel, were used to simulate blurred images. Additive Gaussian white noises with standard deviations  $\sigma_n = \sqrt{2}$  were then added to the blurred images, respectively.

In the first step, we applied the CSR and ASDS-AR for ORL databases, then, we take these results and we implement them using different face recognition methods.

We compare all results obtained during the simulation in order to have Error Equal Rate (EER) values and recognition rate relative to rank for both methods ASDS-AR and CSR.

All results were summarized in table 1, table 2, table 3 and table 4. In addition, a visual comparison of different methods mentioned previously is presented in figures 4 to 7. i. It can be seen from tables 1 to 4 that Gabor linear discriminant analysis (GLDA) gives the best overall performance comparing with all algorithms used in this study. In the first case (9x9 uniforms blur  $\sigma_n = \sqrt{2}$ ), the rank one recognition rate and equal error rate of GLDA are equal to 92.50% and 3.26% respectively using centralized sparse representation, higher than that of all algorithms presented in the tables 1 and 2. ii. In the second case (Gaussian blur with standard deviation 3), the rank one recognition rate and equal error rate of GLDA are equal to 91.65% and 3.33% respectively using centralized sparse representation, higher than that of all algorithms presented in the tables 3 and 4.

Figures 4 and 6 plot the evaluation of the performance of all algorithms, using centralized sparse representation (CSR) and adaptive sparse domain selection with adaptive regularization (ASDS-AR) of ORL database. The comparative results of face recognition algorithms are presented in form of CMC curves. Here KFA, KPCA, LDA, PCA and their combination with Gabor wavelet and Phase congruency were adopted for the comparison. In addition to graphical results, figures 5 and 7, we also present the ROC curves for all algorithms used in this work.

First Case: 9x9 uniform blur  $\sigma_n = \sqrt{2}$

Table-1

Rank one recognition rate (in %)

Methods	KFA	KPCA	LDA	PCA	GKFA	GKPCA	<b>GLDA</b>	GPCA	PCKFA	PCKPCA	PCLDA	PCPCA
CSR	86.79	47.86	87.14	62.50	92.50	76.67	<b>92.50</b>	75.83	83.33	66.67	85.83	64.17
ASDS-AR	88.21	47.86	86.79	61.07	91.67	79.17	<b>92.50</b>	79.17	81.67	70.83	85.83	60.83

Table-2

Equal Error Rate "EER" (in %)

Methods	KFA	KPCA	LDA	PCA	GKFA	GKPCA	<b>GLDA</b>	GPCA	PCKFA	PCKPCA	PCLDA	PCPCA
CSR	6.80	8.93	4.65	5.37	3.43	4.86	<b>3.26</b>	3.33	7.32	5.83	5.96	6.61
ASDS-AR	7.11	9.29	4.73	5.44	3.45	5.00	<b>3.33</b>	3.51	6.65	5.65	6.67	6.62

Second Case : Gaussian blur with standard deviation 3

Table-3

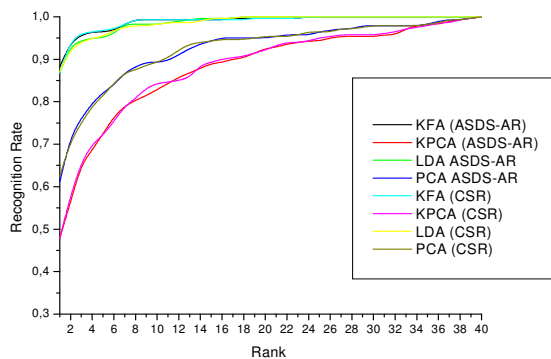
Rank one recognition rate (in %)

Methods	KFA	KPCA	LDA	PCA	GKFA	GKPCA	<b>GLDA</b>	GPCA	PCKFA	PCKPCA	PCLDA	PCPCA
CSR	86.07	47.79	88.21	53.21	90.83	72.50	<b>91.65</b>	73.33	80.00	65.83	81.67	65.83
ASDS-AR	79.29	33.93	87.50	40.36	78.33	36.67	<b>84.17</b>	65.00	81.67	47.50	72.50	61.67

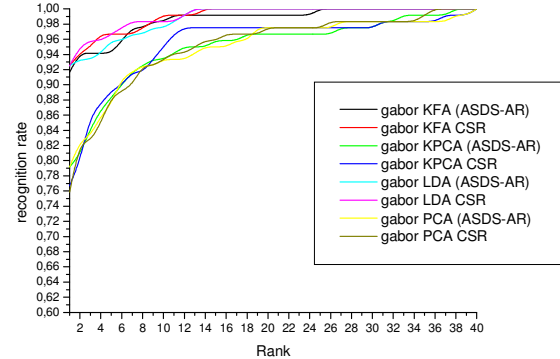
Table-4

Equal error rate (in %)

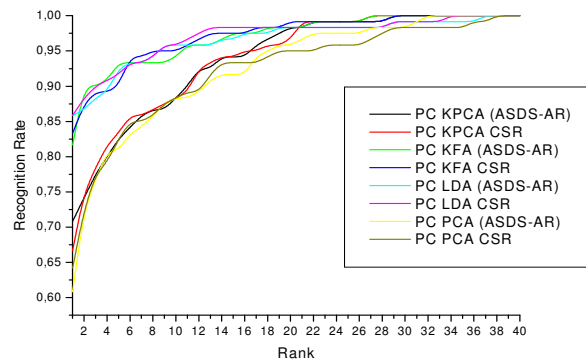
Methods	KFA	KPCA	LDA	PCA	GKFA	GKPCA	<b>GLDA</b>	GPCA	PCKFA	PCKPCA	PCLDA	PCPCA
CSR	6.50	8.24	4.29	6.13	4.17	5.05	<b>3.33</b>	3.33	8.35	7.51	6.66	9.18
ASDS-AR	13.92	7.14	4.64	8.20	5.84	11.66	<b>3.43</b>	5.01	8.33	10.82	8.33	8.34



(a) Without PC and Gabor wavelet

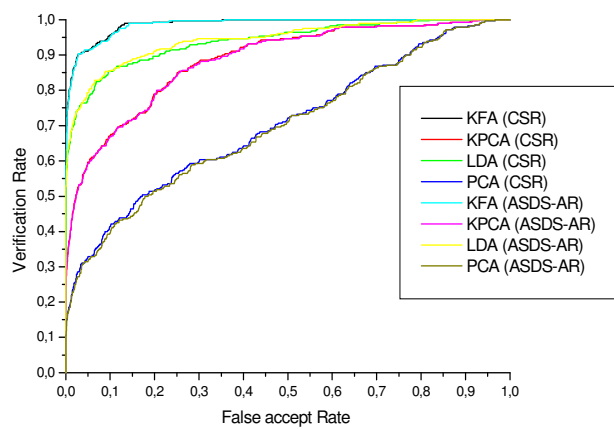


(b) combination with Gabor wavelet

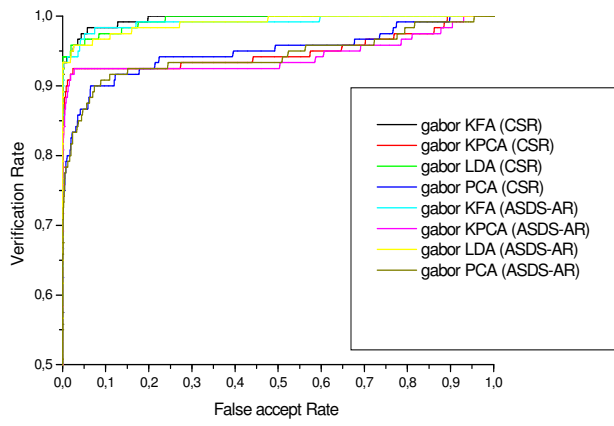


(c) Combination with phase congruency  
Figure-4

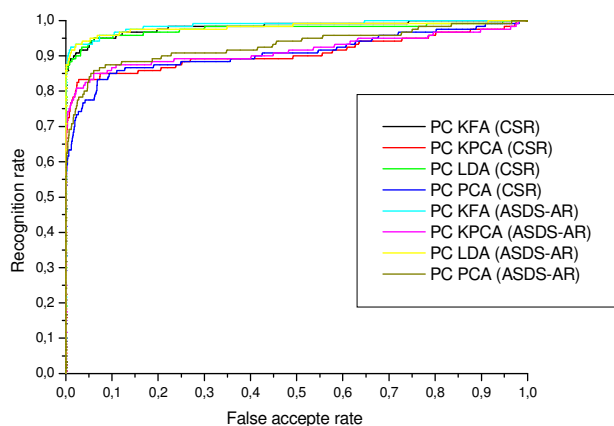
CMC Comparison curves obtained with different algorithms using 9x9 uniform blur  $\sigma_n = \sqrt{2}$



(a) Without PC and Gabor wavelet

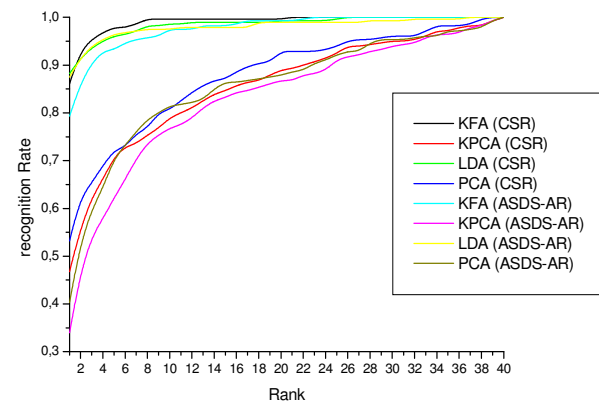


(b) combination with Gabor wavelet

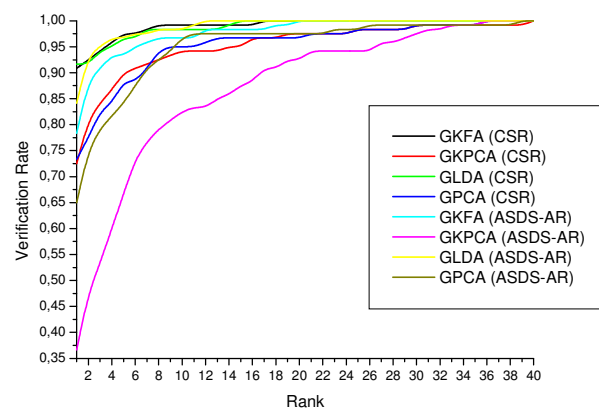


(c) Combination with phase congruency  
Figure-5

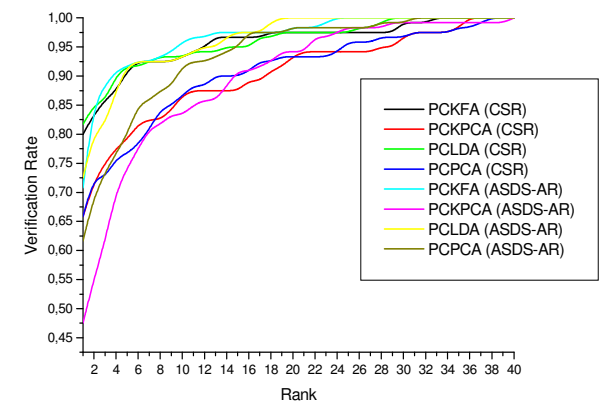
ROC Comparison curves obtained with different algorithms using  $9 \times 9$  uniform blur  $\sigma_n = \sqrt{2}$



(a) Without PC and Gabor wavelet

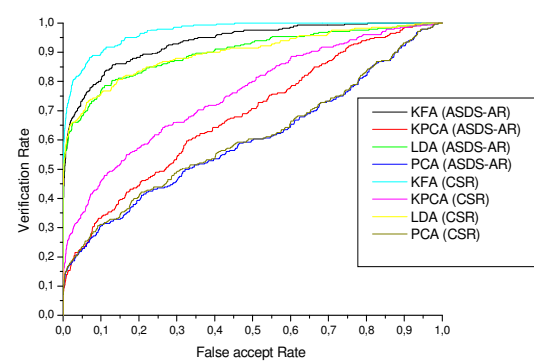


(b) combination with Gabor wavelet

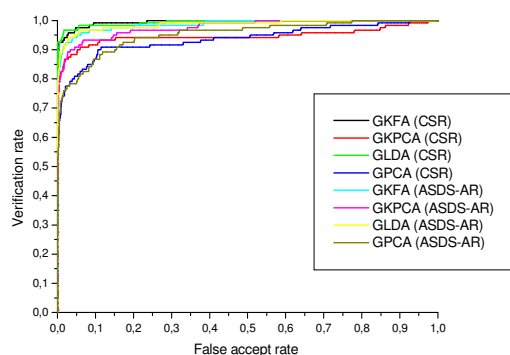


(c) Combination with phase congruency

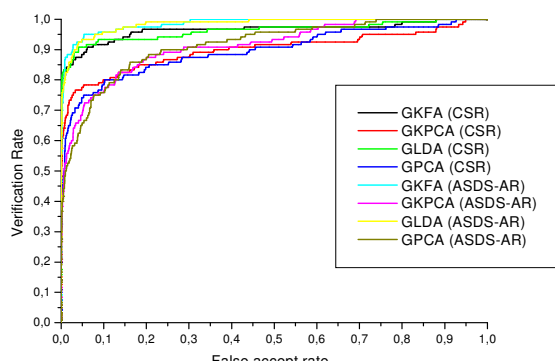
Figure-6  
CMC\_Comparison curves obtained with different algorithms using Gaussian blur with standard deviation 3



(a) Without PC and Gabor wavelet



(b) Combination with Gabor wavelet



(c) Combination with phase congruency

**Figure-7**

#### CMC Comparison curves obtained with different algorithms using Gaussian blur with standard deviation 3

The experimental results show that the Gabor wavelet gives better results than the Phase Congruency method in terms of face recognition rate. Furthermore, the values of EER are more important when using the Gabor Wavelets i.e. values of EER when we use Gabor wavelets is smaller than EER Phase congruency. Secondly, the CSR is more effective than ASDS-AR in terms of face restoration shown in Tables 1 to 4.

Our experimental results suggest that Gabor linear discriminant analysis (GLDA) ensures the most consistent verification rates across the tested ORL databases for both methods CSR and ASDS-AR.

## Conclusion

We presented an empirical evaluation of the popular appearance based feature extraction algorithms within face recognition system based on image face deblurring. The tested algorithms used in this research (KFA, KPCA, LDA, PCA, GKFA, GKPCA, GLDA, GPCA, PCKFA, PCKPCA, PCLDA and PCPCA) were evaluated using the ORL databases, created using centralized sparse representation (CSR) and adaptive sparse domain selection with adaptive regularization (ASDS-AR). The selected tests are divided on three steps, in the first, we used directly the following face recognition methods (LDA, KFA, PCA, and KPCA) and in the second, we associated them with the Gabor wavelet and in the third, we related them with the Phase Congruency.

Our experiments suggest that when we associate the Gabor wavelet gives better results than Phase Congruency. In addition, Centralized Sparse Representation (CSR) has proven its effectiveness in image face deblurring compared with Adaptive Sparse Domain Selection and Adaptive Regularization (ASDS-AR). However, among the methods tested, GLDA was judged the best achieving the lowest error rate compared to other methods.

## Acknowledgement

The authors are thankful to the members of laboratory LMSS and LEMI of Boumerdes University, without forgetting the editorial board and reviewers for their valuable suggestions.

## References

- Li S.Z. and Jain. A.K., editors. *Handbook of Face Recognition*. SpringerVerlag, New York, (2005)
- Nishiyama M., Takeshima H., Shotton J., Kozakaya. T., and Yamaguchi. O., Facial deblur inference to improve recognition of blurred faces. *Proc. CVPR*, 1115– 1122 (2009)
- Ramponi. G and cubic. A, unsharp masking technique for contrast enhancement, *Signal Processing*, 67(2), 211–222 (1998)
- Ramponi. G and Polesel. A, Rational unsharp masking technique. *Journal of Electronic Imaging*, 7(2), 333–338 (1998)
- Chan. T.G and Wong C. K.. Total variation blind deconvolution. *IEEE Trans. on Image Processing*, 7(3), 370–375 (1998)
- Yao. Y, Abidi. B and Abidi. M, Quality Assessment and

- Restoration of Face Images in Long Range/High Zoom Video (*Chap 4*), Springer, Berlin, 43–60 (2007)
7. Struc. V, Pavesic. N, Gabor-based kernel partial-least-squares discrimination features for face recognition, *Informatica*, **2** (20), 115–138 (2009)
8. Struc. V, Pavesic. N., The complete Gabor-Fisher classifier for robust face recognition, *EURASIP. Journal of Adv Signal Process, article ID 847680*, (2010)
9. Batagelj B. and Solina F., Face recognition in different subspaces – a comparative study, in *Proc. of the 6th International Workshop on Pattern Recognition in Information Systems, PRIS'06*, 71–80 (2006)
10. Esbati H. and Shirazi J., face recognition with PCA and KPCA using Elman neural network and SVM, *world academy of science engineering and technology*, **5** (52), 174-178 (2011)
11. Baochang Z., Gabor-kernel fisher analysis for face recognition, *In Proc of PCM* (2), 802–809 (2004)
12. Chan C., Kittler J. and Messer K., Multi-scale local binary pattern histograms for face recognition, in *Proc. Int. Conf. Biometrics*, 809–818 (2007)
13. Shen. L, Bai. L. Bardsley. D and Yangsheng. W Gabor feature selection for face recognition using improved adaboost learning. *In Proc of IWBRIS*, 39–49 (2005)
14. Y. Su, Shiguang. S, Xilin C, and Wen. G. Multiple fisher classifiers combination for face recognition based on grouping adaboosted gabor features, *In Proc of BMVC*, (2006)
15. Zahra M. Image Duplication Forgery Detection using Two Robust Features. *Res J. of Recent Sci.* **1**(12), 1-6 (2012)
16. Laurenz W, Fellous. J. M, Kruger. N, and Malsburg. C. D. Face recognition by elastic bunch graph matching. *IEEE Trans. On Pattern Analysis and Machine Intelligence*, **19**(7), 775–779 (1997)
17. Zhang B., Shan S., Chen X. and Gao W., Histogram of Gabor phase patterns: A novel objects representation approach for face recognition, *Image Processing, IEEE Transactions on*, **16**(1), 57–68 (2007)
18. Hong L., Jain A, Pankanti S and Bolle R., Fingerprint enhancement. In *Proceedings of the 1st IEEE WACV, Sarasota*, 202–207 (1996)
19. Wiskott L., Fellous J.M., Kruger N., Malsburg C.V., Face recognition by elastic bunch graph matching, *IEEE Trans on Pattern Analysis & Machine Intel*, **8**(19), 775–779 (1997)
20. Kong W.K., Zhang D. and Li W., Palmprint feature extraction using 2-D Gabor filters, *Patt Recog*, **36**(10), 2339–2347 (2003)
21. Kovesi P., Image features from phase congruency, *Videre: J. of Computer Vision Res*, **1**(3), 1–26 (1999)
22. Venkatesh. S and Owens. R., An energy feature detection scheme, in *Proceedings of the International Conf on Image Proces. 553–557, Singapore*, (1989).
23. Patheja P.S., Akhilesh.W A. and Maurya J. P. An Enhanced Approach for Content Based Image Retrieval, Features, *Res J. of Recent sci.*, **1**(ISC-2011), 415-418 (2012)
24. Dong W., Zhang L. and Shi G., Centralized sparse representation for image restoration, *in Proc of the IEEE (ICCV), Barcelona* (2011)
25. Elad M., Sparse and Redundant Representations: From Theory to Applications in Signal and Image Processing, in: Springer (Eds.), Iterative-Shrinkage Algorithms, 111–138 (2010)
26. Dong. W, Zhang. L, Shi. G. and. Wu. X, Image deblurring and super-resolution by adaptive sparse domain selection and adaptive regularization, *IEEE Trans Image Process*, **20**(7), 1838–1857 (2011)